

Study of combined natural convection-surface radiation with internal heat generation

Saber Hamimid *Messaoud Guellal

Laboratory of Chemical Engineering – Faculty of Engineering, University Setif 1, Algeria

Abstract

In the present work, two-dimensional simulation of the effects of radiation on natural convection flow in a square cavity whose four walls have the same emissivity, in the presence of heat generation have been investigated. The surface emissivity ε , the external Rayleigh number Ra_E , the internal Rayleigh number Ra_I and the radiation number Nr were varied parametrically. Finite volume method through the concepts of staggered grid and SIMPLER algorithm has been applied, and the view factors were determined by analytical formula. A power scheme was also used in approximating advection–diffusion terms. Representative results illustrating the effects of emissivity and the internal heat generation on the streamlines and temperature contours within the enclosure are reported. In addition, results for local and average convective and radiative Nusselt number are presented and discussed for various parametric conditions.

Key words: Natural convection, surface radiation, Internal heating, Numerical simulation

1. Introduction

Due to its many engineering applications and impact on flow structure and heat transfer processes in double pane windows, solar collectors, building insulation, nuclear engineering, ovens and rooms; combined natural convection and radiation exchange between surfaces involving a radiatively non-participating medium inside enclosures has been a very important research topic. During the last four decades, significant attention was given to the study of natural convection in enclosures subjected to volumetric internal heat generation, ranging from the mantle convection in the earth [1,2] to the cooling of a molten nuclear reactor core [3,4]. However, the interaction between natural convection and surface radiation is rarely studied although surface radiation is inherent in natural convection.

Many studies on laminar and turbulent natural convection heat transfer in a rectangular enclosure are carried out including radiation [5–10].

In the present work, two-dimensional unsteady simulation of the effects of radiation on natural convection flow in a square cavity whose four walls have the same emissivity, in the presence of heat generation have been investigated. The surface emissivity ε , the external Rayleigh number Ra_E , the internal Rayleigh number Ra_I (or the external to internal Rayleigh number $Ra_{EI} = Ra_E / Ra_I$) and the radiation number Nr were varied parametrically

*Corresponding author: Address: Faculty of Technology, Laboratory of Chemical Engineering, University of Setif-1, 19000, Setif, ALGERIA. E-mail address: messaoud.guellal@gmail.com, Phone: +213561288921 Fax: +21336611189

2. Mathematical formulation

The flow is assumed to be incompressible, laminar and two dimensional in an enclosure of square cavity with internal heat generation, the two vertical walls are maintained at two different temperatures T_H and T_C , while the two horizontal walls are submitted to a radiative heat flux $q_r = k \frac{\partial T}{\partial y}$. It will be further assumed that the temperature differences in the domain under consideration are small enough to justify the employment of the Boussinesq approximation such as:

$$\rho = \rho_0[1 - \beta(T - T_0)] \quad (1)$$

The fluid is air and its properties are assumed constant at the average temperature T_0 , except for the density whose variation with the temperature is allowed in the buoyancy term. The inner surfaces, in contact with the fluid, are assumed to be gray, diffuse emitters and reflectors of radiation with identical emissivities.

The governing equations for this problem are based on the balance laws of mass, linear momentum and energy. Taking into account the assumptions mentioned above, the governing equations for the problem in two dimensions unsteady states can be written in dimensionless form as:

$$\frac{\partial U}{\partial X} + \frac{\partial V}{\partial Y} = 0 \quad (2)$$

$$\frac{\partial U}{\partial \tau} + U \frac{\partial U}{\partial X} + V \frac{\partial U}{\partial Y} = -\frac{\partial P}{\partial X} + \text{Pr} \left(\frac{\partial^2 U}{\partial X^2} + \frac{\partial^2 U}{\partial Y^2} \right) \quad (3)$$

$$\frac{\partial V}{\partial \tau} + U \frac{\partial V}{\partial X} + V \frac{\partial V}{\partial Y} = -\frac{\partial P}{\partial Y} + \text{Pr} \left(\frac{\partial^2 V}{\partial X^2} + \frac{\partial^2 V}{\partial Y^2} \right) + Ra \text{Pr} \theta \quad (4)$$

$$\frac{\partial \theta}{\partial \tau} + U \frac{\partial \theta}{\partial X} + V \frac{\partial \theta}{\partial Y} = \left(\frac{\partial^2 \theta}{\partial X^2} + \frac{\partial^2 \theta}{\partial Y^2} \right) + \frac{Ra_I}{Ra_E} \quad (5)$$

Ra_E and Ra_I are the external and the internal Rayleigh numbers defined respectively as:

$$Ra_E = g \beta \Delta T H^3 / (\nu \alpha)$$

$$Ra_I = g \beta q H^5 / (\nu \alpha k)$$

The corresponding initial and boundary conditions are :

$$\begin{aligned}
U=V=0, \quad \theta &= \theta_i && \text{for } \tau=0 \\
U=V=0, \quad \theta &= \theta_c = -0.5 && \text{for } 0 \leq Y \leq 1 \text{ at } X=0 \\
U=V=0, \quad \theta &= \theta_h = 0.5 && \text{for } 0 \leq Y \leq 1 \text{ at } X=1 \\
U=V=0, \quad \frac{\partial \theta}{\partial Y} - Nr Q_r &= 0 && \text{for } 0 \leq X \leq 1 \text{ at } Y=0 \\
U=V=0, \quad \frac{\partial \theta}{\partial Y} - Nr Q_r &= 0 && \text{for } 0 \leq X \leq 1 \text{ at } Y=1
\end{aligned}$$

Where $Nr = \sigma T_0^4 H / k \Delta T$, is the dimensionless parameter of conduction-radiation and $Q_r = q_r / \sigma T_0^4$, is the dimensionless net radiative heat flux.

Therefore, the dimensionless net radiative flux density along a diffuse-gray and opaque surface “ A_i ” is expressed as:

$$Q_{r,i} = R_i - \sum_{j=1}^N R_j F_{i-j} \quad (6)$$

R_i is the dimensionless radiosity of surface A_i , obtained by resolving the following system:

$$\sum_{j=1}^N (\delta_{ij} - (1 - \varepsilon_i) F_{i-j}) R_j = \varepsilon_i \Theta_i^4 \quad (7)$$

Where the dimensionless radiative-temperature Θ_i is given by

$$\Theta_i = \frac{T_i}{T_0} = [(T_h - T_c) \theta_i + T_0] / T_0 = \theta_i \frac{\Delta T}{T_0} + 1 \quad (8)$$

$$\Theta_i = \frac{\theta_i}{\theta_0} + 1 \quad (9)$$

3. Numerical procedure

The numerical solution of the governing differential equations for the velocity, pressure and temperature fields is obtained by using a finite volume technique. A power scheme was also used in approximating advection–diffusion terms. The SIMPLER algorithm (Semi-Implicit Method for Pressure Linked Equations Revised) whose details can be found in Patankar [11], with a staggered grid is employed to solve the coupling between pressure and velocity. The governing equations were cast in transient form and a fully implicit transient differencing scheme was employed as an iterative procedure to reach steady state. The discretised equations are solved using the line by line Thomas algorithm with two directional sweeps.

The radiosities of the elemental wall surfaces are expressed as a function of elemental wall surface temperature, emissivity and the shape factors. The radiosity (R_i) and temperature (θ_i) are connected by equation (18) whose resolution is performed by the Gauss elimination method.

In 2D, the view factors are analytic [12] :

$$F_{ij} = \frac{-1}{2(x_2 - x_1)} \left[\sqrt{x_2^2 + y^2} \Big|_{y_1}^{y_2} - \sqrt{x_2^2 + y^2} \Big|_{y_1}^{y_2} \right] \quad (10)$$

$$F_{i-k} = -\frac{1}{2(x_2 - x_1)} \left[\sqrt{(x_2 - x)^2 + H^2} \Big|_{x=x_1}^{x=x_2} - \sqrt{(x_1 - x)^2 + H^2} \Big|_{x=x_1}^{x=x_2} \right] \quad (11)$$

In order to obtain good convergence solutions, the convergence criterion for the residuals was set at 10^{-5} .

The outer iterative loop is repeated until the steady state is achieved which occurs when the following convergences are simultaneously satisfied: $|\phi_{ij}^{old} - \phi_{ij}| \leq \varepsilon_\phi$, where ϕ represents the variables U, V or θ . In most of the cases, the velocity components and temperatures were driven to $\varepsilon_U = \varepsilon_V = \varepsilon_\theta \leq 10^{-6}$.

4. Discussion

This section is devoted to analyse the effects of the internal heat generation parameter (Ra_i) on the flow and heat transfer on the combined natural convection surface radiation flow considering $Ra_E = 10^6$, $\varepsilon = (0.2, 0.5)$ and $\Delta T = 10k$.

For low Ra_i ($\leq 10^7$), considerations are given to the cases when the effects of external heating and internal heat generation are comparable. Figures 1 illustrates the sequences of flow and thermal fields for $\varepsilon = 0.2$ and $\varepsilon = 0.5$ respectively. Performing order of magnitude analysis for $Ra_i = 0$ and $Ra_i = 10^6$ implies that the relative impact of internal heat generation is minor. The flow is attributed by the presence of a single clockwise circulation cell, which occupies much of the cavity and a secondary and a tertiary vortices are formed inside the cavity (vortices of surface radiation effects without internal heat generation, $Ra_i = 0$).

As the heat generation increases, ($Ra_i \geq 10^7$), the total thermal energy in the cavity is on increase, those small vortices are merged to the primary vortex of relatively higher intensity of circulation than that at low Ra_i .

Consequently, a counter-clockwise small cell appeared at the upper left corner (for $Ra_i = 2 \times 10^7$), and is shifted left with increasing Ra_i . The flow strength in this new cell also increases when the internal heat generation increases in magnitude.

For large values of internal Rayleigh number, the whole cavity is occupied by two recirculating cells; i.e. both counter-clockwise and clockwise cells near the hot and cold side walls respectively due to the positive buoyancy effect. The isotherms tend to be horizontally uniform and vertically linear at the upper portion of the enclosure. However, in the bottom part of the cavity, the isotherms are divided into two groups.

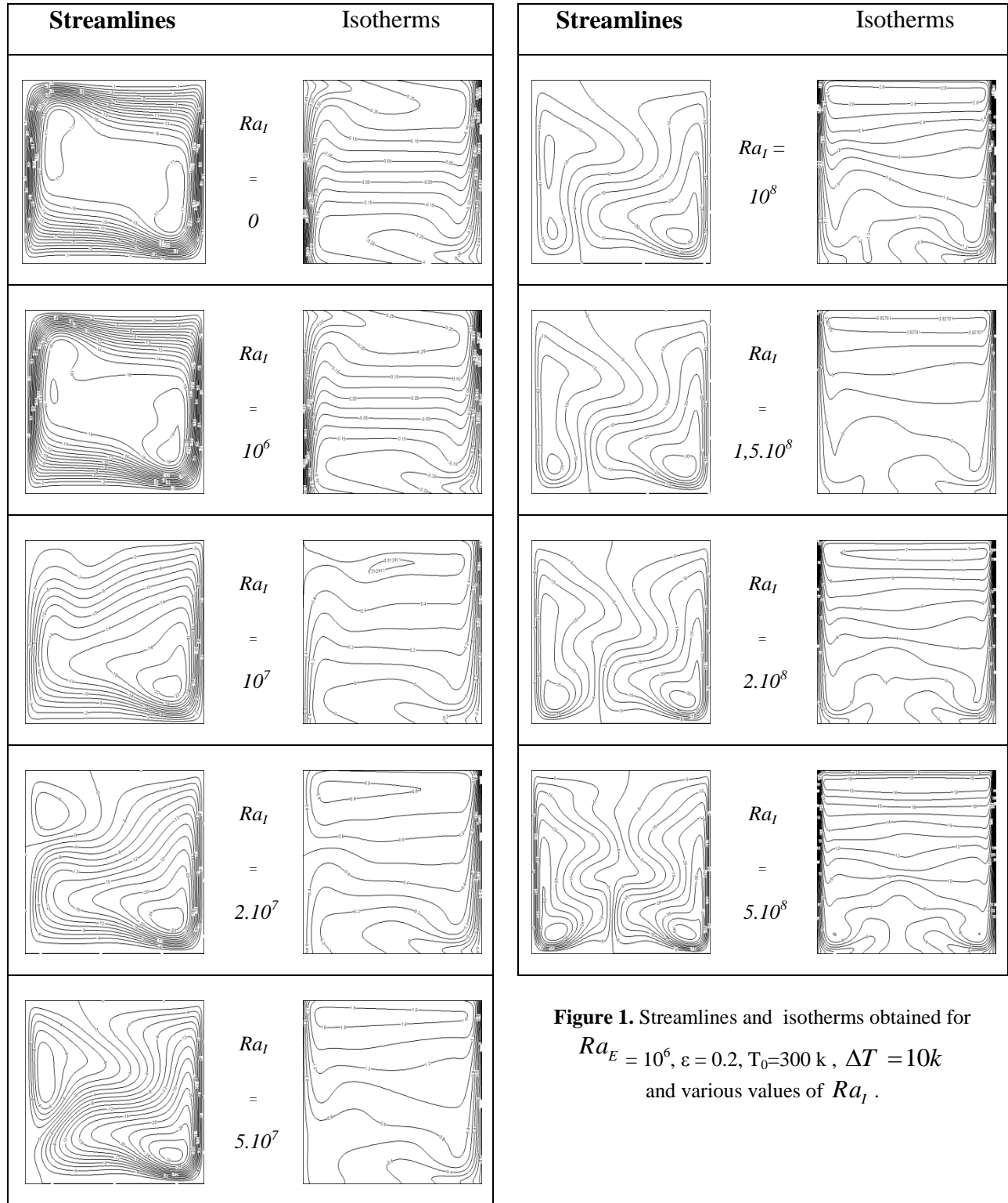


Figure 1. Streamlines and isotherms obtained for $Ra_E = 10^6$, $\varepsilon = 0.2$, $T_0 = 300 \text{ K}$, $\Delta T = 10 \text{ K}$ and various values of Ra_1 .

This effect of internal heat generation on the flow field is reasonable since internal heat generation assists buoyancy forces by accelerating the fluid flow, (Figures 2a, 2b and 2c).

On other hand, the presence of heat source within the enclosure causes an increase in the fluid temperature, (Figure 2d), leading to a reduction of convective and radiative heat transfer on the hot wall (Figures 3 and 4).

From figures 3 and 4, we can also note that for weak heat generation, local convective and radiative Nusselt numbers have positive values, and from $Ra_l = 2.10^7$ all values are negative. This means that, the heat is transferred from the fluid to the hot wall (the hot wall absorbs the heat from the interior higher temperature fluid). The negative sign of Nu_c and Nu_r corresponds to the apparition of the small counter-clockwise cell shown previously in figure 1. It is noticeable that the absolute value for the temperature gradient has a maximum value at this position, since this cell is coming to the hot wall at the upper corner; so therefore, the values of Nu_c and Nu_r along the hot side wall are governed by the direction and strength of the flow adjacent to the hot wall.

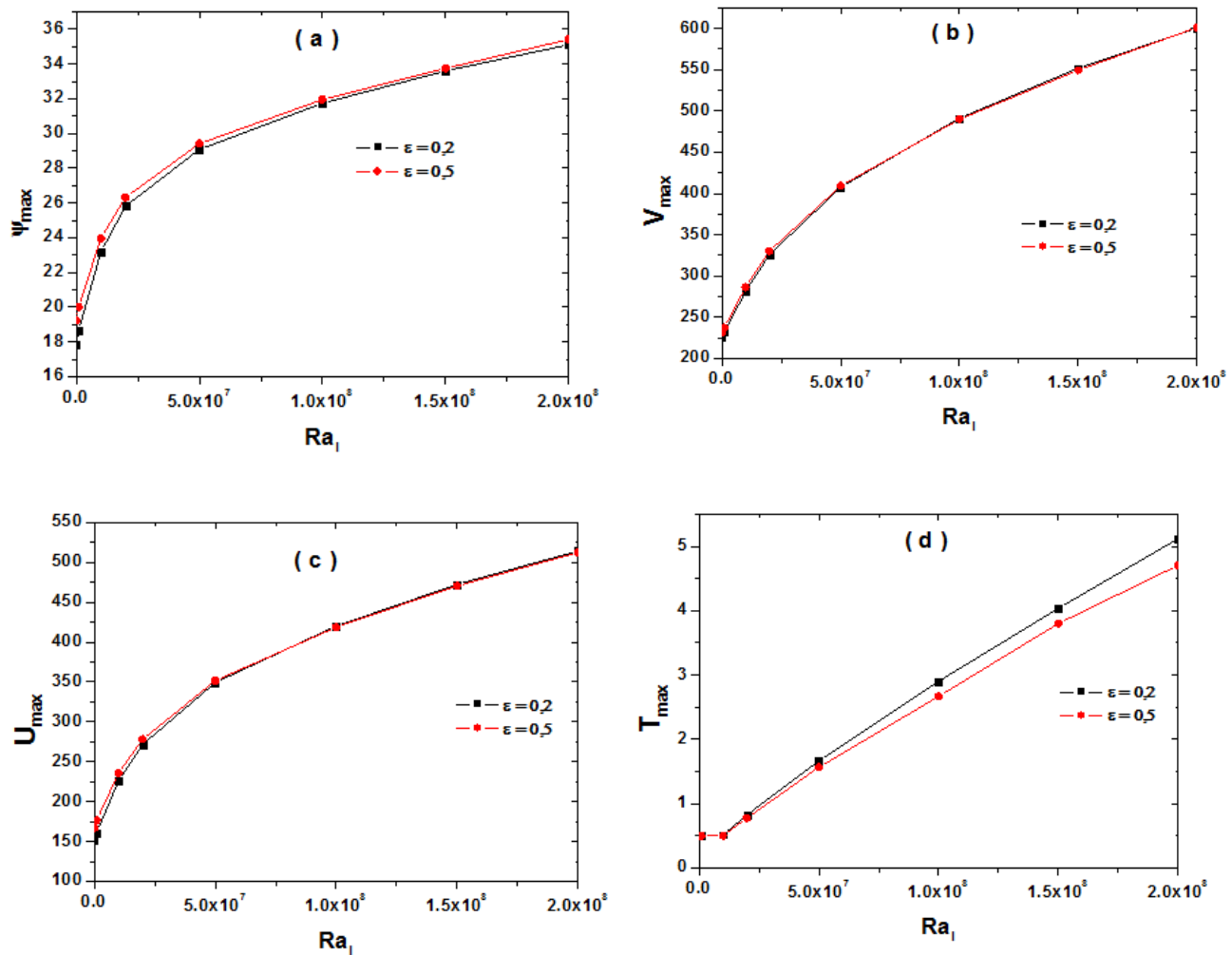


Figure 2. Maximum values of the stream function (a), vertical velocity (b), horizontal velocity(c) and temperature (d) field variation with internal Rayleigh number for $Ra_E = 10^6$ and various emissivity ε .

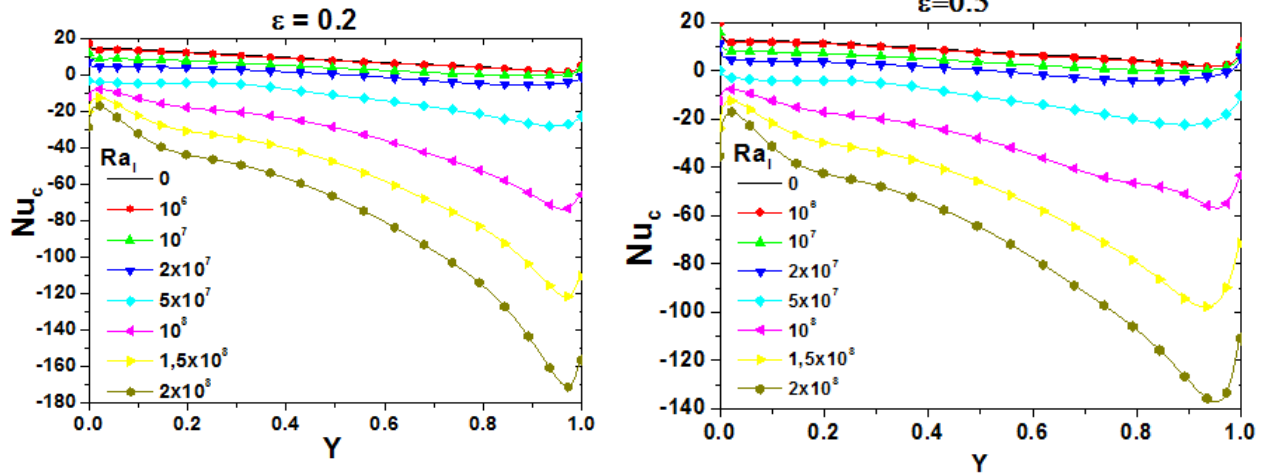


Figure 3. Local convection Nusselt number on the hot wall for $Ra_E = 10^6$

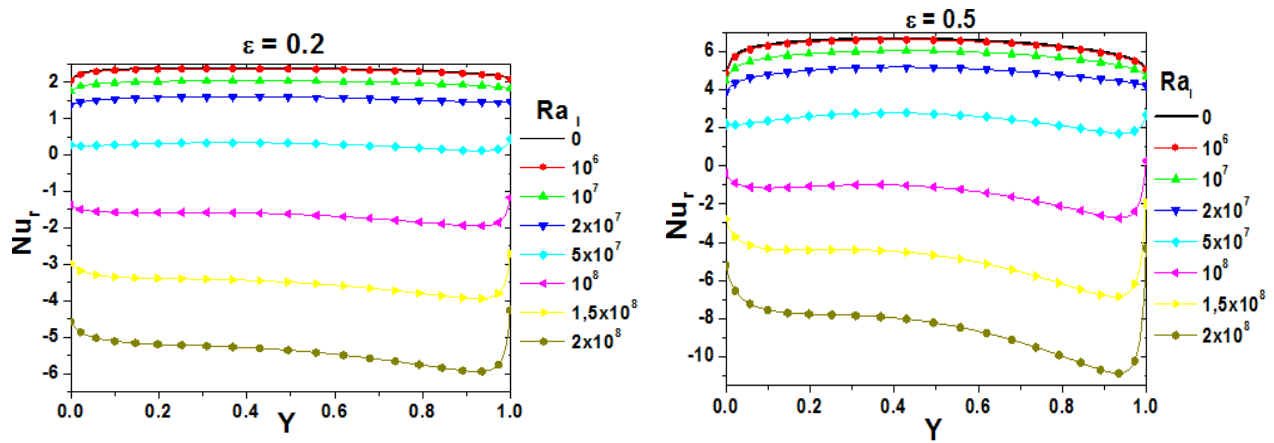


Figure 4. Local radiation Nusselt number on the hot wall for $Ra_E = 10^6$

Figure 5 illustrates the variation of average convective and radiative Nusselt numbers for different values of internal heat generation and emissivity. The positive value of $Nu_{c,avg}$ and $Nu_{r,avg}$ marks that there is ascending motion near the hot wall though the circulation feels retardation due to the buoyancy effect generated by internal heat generation. Therefore, as Ra_i increases, the average convective and radiative Nusselt numbers decrease indicating the descending motion near the hot side wall.

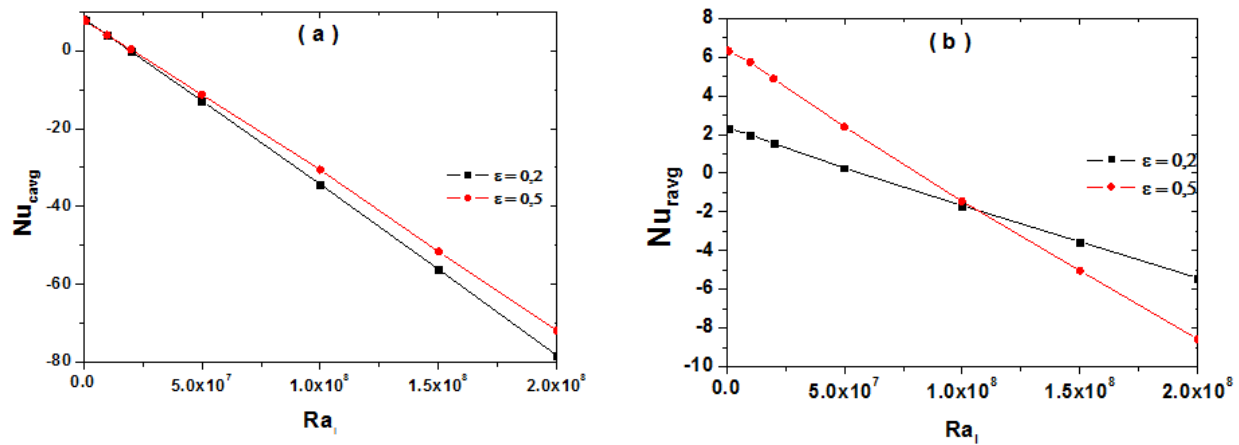


Figure 5. Variations of the average convection (a) and radiation (b) Nusselt number as a function of Ra_i

for $Ra_E = 10^6$ and $\Delta T = 10K$.

Conclusions

Combined natural convection and surface radiation in a differentially-heated cavity in the presence of internal heat generation has been numerically studied. The obtained results reveal that the increase in the value of the heat generation parameter leads to increase in the flow rates in the secondary cell and therefore an increase in its size until it occupies the half of the total cavity space. Supplementary increasing of heat generation causes a development of more cells in the cavity.

The temperature of the fluid in the cavity also increases due to the augmentation of internal heat generation and hence that negates the heat transfer from the heated surface.

Nomenclature

A_i	radiative surface number i	Q_r	dimensionless net radiative-flux, $q_r / \sigma T_0^4$
F_{i-j}	view-factor between the surfaces A_i and A_j	q_r	net radiative flux ($W \cdot m^{-2}$)
g	gravitational acceleration, $m \cdot s^{-2}$	q	internal heat generation ($W \cdot m^{-3}$)
H	height of the enclosure, m	Ra_E	External Rayleigh number,
k	thermal conductivity, $W \cdot m^{-1} \cdot K^{-1}$	Ra_i	Internal Rayleigh number
Nr	radiation number, $\sigma T_0^4 (k \Delta T / H)$	R_i	dimensionless radiosity
Nu_c	Convective Nusselt number	T	dimensional temperature, K
Nu_r	Radiative Nusselt number	T_0	Reference temperature, $(T_C - T_H) / 2$, K,

P	dimensionless pressure,	U, V	dimensionless velocity-components,
Pr	Prandtl number, ν / α .	X, Y	dimensionless coordinates
	<u>Greek symbols</u>	Θ	dimensionless temperature, T / T_0
α	thermal diffusivity, $m^2.s^{-1}$	τ	dimensionless time
β	thermal expansion coefficient, K^{-1}		<u>Subscripts</u>
ΔT	temperature difference, K	max	maximum value
ε_i	emissivity of surface A_i	0	reference state
ν	kinematic viscosity, $m^2.s^{-1}$	C	cold
ρ	fluid density, $Kg.m^{-3}$	H	hot
σ	Stefan–Boltzmann constant, $W.m^{-2}.K^{-4}$	c	convective
θ	dimensionless temperature, $(T - T_0) / \Delta T$.	r	radiative

References

- [1] McKenzie DP, Roberts JM, Weiss NO. Convection in the earth's mantle: toward a numerical simulation, J Fluid Mech 1974;62:465–538.
- [2] Travis B, Weinstein S, Olson P, Three-dimensional convection planforms with internal heat generation, Geophys Res Lett 1990;17:243–246.
- [3] Sharmaa A, Velusamy K, Balajib C, Conjugate transient natural convection in a cylindrical enclosure with internal volumetric heat generation. Ann Nucl Energ 2008;1502-1514
- [4] Lee SD, Lee JK, Suh KY, Natural convection thermo fluid dynamics in a volumetrically heated rectangular pool, Nucl Eng Des 2007;237:473–483.
- [5]. Balaji C, Venkateshan SP, Combined surface radiation and free convection in cavities, J Thermophys Heat Transfer 1994;8:373–376.
- [6] Ramesh N, Venkateshan SP, Effect of surface radiation on natural convection in a square enclosure, J Thermophys Heat Transfer 1999;13:299–301.
- [7] Velusamy K, Sundararajan T, Seetharamu K, Interaction effects between surface radiation and turbulent natural convection in square and rectangular enclosures, J Heat Transfer 2001;123:1062–1070.
- [8] Anil KS, Velusamy K, Balaji C, Venkateshan SP, Conjugate turbulent natural convection with surface radiation in air filled rectangular enclosures, Int J Heat Mass Transfer 2007;50:625–639.
- [9] Alvarado R, Xamán J, Hinojosa J, Álvarez G, Interaction between natural convection and surface thermal radiation in tilted slender cavities, Int J Thermal Sciences 2008;47:355–368.
- [10] Xamán J, Arce J, Álvarez G and Chávez Y, Laminar and turbulent natural convection combined with surface thermal radiation in a square cavity with a glass wall. Int J Thermal Sciences 2008;47: 1630–1638
- [11] Patankar SV, Numerical heat transfer and fluid flow, New York: McGraw-Hill; 1980.

- [12] Howell JR, A Catalogue of Radiation Configuration Factors, New York: McGraw-Hill; 1982.